THE JOURNAL OF PHYSICAL CHEMISTRY B

ARTICLE

pubs.acs.org/JPCB

Effects of Concentration and Temperature on the Dynamic Behavior of PAA-*g*-PEO Aqueous Solutions with Different Counterion Species: A Dielectric Spectroscopy Study

Chunyan Liu and Kongshuang Zhao*

College of Chemistry, Beijing Normal University, Beijing 100875, China

ABSTRACT:

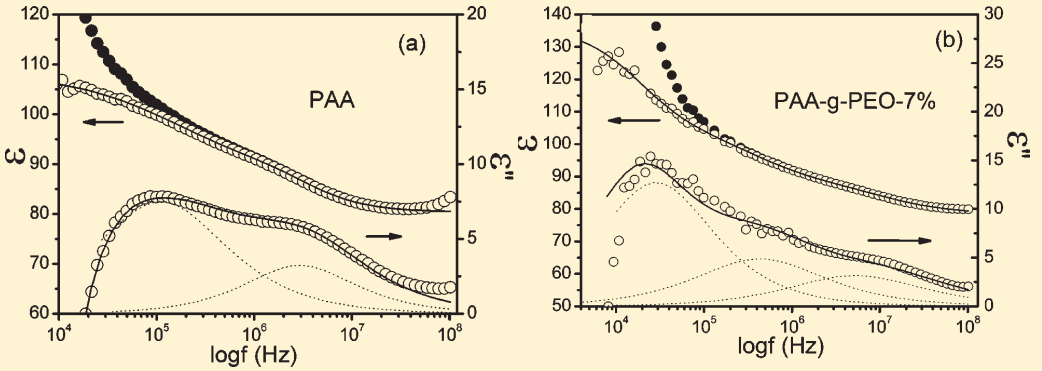

Dielectric properties of PAA-*g*-PEO-7% solutions with different counterions were measured as a function of concentration and temperature over a frequency range of 40 Hz to 110 MHz. After the contribution of electrode polarization effects was subtracted, the dielectric spectra of PAA-*g*-PEO-7% solutions showed three relaxation processes in the experimental frequency range, named low-, mid-, and high-frequency relaxation. The observed three relaxations were strictly analyzed by using the Cole−Cole relaxation function, and the dielectric parameters (dielectric increment $\Delta\varepsilon$ and the relaxation time τ) were obtained. The scaling relation of dielectric increment and relaxation time of high frequency with concentration C_p were obtained and compared with the predictions of scaling theories. The information on the dynamics and microstructure of PAA-*g*-PEO-7% was obtained. Using different counterion species, the mid- and high-frequency relaxation mechanisms were attributed to the fluctuation of condensed counterions and free counterions, respectively, and the low-frequency relaxation was considered to be caused by the interface polarization of a complex formed by the hydrogen bonding between carboxylic group of PAA and ether oxygen on the side-chain PEO. In addition, by means of Eyring equation, the thermodynamic parameters, enthalpy change ΔH and entropy change ΔS, of the three relaxations were calculated from the relaxation time and discussed from the microscopic thermodynamical view.

1. INTRODUCTION

Dynamic behavior of polyelectrolyte solutions, which depend on the structure, conformation of chains, and electrostatic interaction, have attracted increasing attention.[1−3] The strong electrostatic interactions between charges, which are the most typical characteristic of polyelectrolyte, lead to the various behaviors, such as complex chain conformation and charge distribution of polyelectrolyte solutions. Because the electrostatic interactions and dynamics of polyelectrolyte solutions can be described by charge distribution model or ion−dipole interaction, dielectric relaxation spectroscopy (DRS) method is increasingly used for characterizing these interactions, motion of the main or branched chain, and the fluctuation of counterions.[4−6] We have studied the dynamic behaviors of chitosan, a typical biological macromolecule, and poly(diallyldimethylammonium chloride) (PDADMAC) solutions by dielectric spectroscopy coupled with scaling approach.[7−9] In addition, the studies of charged side-chain dynamics in polyelectrolyte aqueous solutions were also reported. For example, the existence of a dielectric dispersion in aqueous solutions of poly(L-glutamic acid) in a region around 100 MHz, attributable to internal motions of the polar groups of the side chains, has been reported by Mashimo et al.[10] and this was later confirmed by Bordi et al.[11] Moreover, the microdynamics of the side chains of poly(lysine) and chitosan derivatives were also reported.[12,13] The above studies showed that DRS is useful for exploring microdynamic information of the charged short side chain in polyelectrolyte solution. But the polyelectrolyte with long and uncharged side chain has not been investigated by DRS; this may be blamed on lack of a suitable model to describe side-chain motion in solution. In this study, the poly(acrylic acid)-*graft*-poly(ethylene oxide) (PAA-*g*-PEO) polyelectrolyte in aqueous solution has the intramolecular hydrogen-bonding interaction between main chain and side chain, which is

Received: October 25, 2011
Published: December 06, 2011

bound to affect the general dynamic behavior of solution. Therefore, by carrying out dielectric analysis coupled with scaling approach and Eyring equation to such a system, the information on counterion motion, the microstructure of PAA-*g*-PEO, conformation transition of chains can be obtained.

Poly(acrylic acid) (PAA), as a weak polyelectrolyte, is used in various fields of engineering and technology flocculants, dispersing agents, the mucoadhesive agents, the drug delivery carriers, etc.[14] Because of its charged structure, the PAA is used as a typical model of the polyelectrolyte solution.[15] PEO, as a water-soluble polymer, was also used in the pharmaceutical field. It was reported that the encapsulation efficiency increased and the release rate was slowed down by attaching PEO chains.[16−18] To decrease water solubility of PAA,[19] novel interpolymer complexes of PAA and methoxy PEO with various molecular weights and compositions, which can promote the adhesive process and slow down the dissolution rate, were prepared.[20−23] Therefore, it is important to obtain the internal dynamics in PAA-*g*-PEO solution for its potential application. The interchain interaction of PAA-*g*-PEO in aqueous solution has been investigated using laser light scattering (LLS), viscometry, and rheological measurements.[24] But it is difficult to get more information on the dynamics and interaction, such as the electrostatic interaction between counterion and fixed charge on polyions and the fluctuation of counterions along the molecular chains, just by any individual method mentioned above but the dielectric measurement.

From a different point of view, the polyelectrolyte, as a soft matter, which is different from those of uncharged polymers, shows typical scaling laws.[25] Ito et al. found that the dielectric parameters show scaling behavior with concentration,[26] and Rubinstein et al. reviewed later the scaling theory of polyelectrolyte solution.[27] Though considerable theoretical work has been devoted to polyelectrolyte solution, the experimental data is relatively backward. In order to obtain the scaling relation between dielectric parameters and concentration experimentally, the dielectric studies were performed in more recent studies as mentioned above.[15,28,29] In addition, the origin of the dielectric relaxation in a frequency range, usually between 1 and 100 MHz, has long been controversial, although many researches considered that it can be ascribed to the fluctuation of free counterions.[26,30,31] To judge the relaxation mechanism in polyelectrolyte solution system, polyelectrolyte solutions with different species of counterions are preferred in this study. On the other hand, the change of the temperature of polyelectrolyte solution, which will affect the molecular movement, the interaction,[32,33] and conformation of chains,[34,35] is an important factor which can help us obtain thermodynamic information.

In this paper, dielectric measurements of the PAA and PAA-*g*-PEO-7% solutions with different counterion species were carried out over the frequency range from 40 Hz to 110 MHz by varying concentration and temperature, respectively. The dielectric spectra which can reflect real dielectric properties of the PAA-*g*-PEO-7% solution were obtained by subtracting the contribution of the electrode polarization, and the characteristic dielectric parameters were also estimated by fitting the real dielectric data. It was found that there are three relaxation processes for the PAA-*g*-PEO-7% solution system, which is one more than for the PAA solution. The micromechanisms of the three relaxations were interpreted separately. In addition, the scaling of the dielectric increment $\Delta\varepsilon$ and the relaxation time τ with the PAA-*g*-PEO-7% concentration C_p were obtained and compared with the predictions of scaling theories. The temperature-dependent characteristic parameters were also analyzed by means of the Eyring equation. Attention was focused on the relaxation mechanism and the influence of temperature and concentration on the dynamical behaviors.

2. EXPERIMENT AND METHODS

2.1. Materials and Preparation of Sample. Poly(acrylic acid) (PAA) (M_w = 2.5 × 10^5 g mol^{-1}) from Sigma-Aldrich was used without further purification. Synthesis of the PAA-*g*-PEO-7% (the weight percent of PEO) was prepared according to the classical reaction of amino with carboxylic groups in the presence of EDC and HOBt, which has been already reported elsewhere.[24] Potassium hydroxide, sodium hydroxide, strong ammonia, potassium chloride, and ethanol from Beijing Chemical Works were analytical grade and used without further purification.

Polymer solutions were prepared by dissolving a known amount of sample in a given volume of doubly distilled water, the specific resistance of which was higher than 16 MΩ·cm^{-1}. The concentration ranged from 5.0 to 0.01 mg·mL^{-1} for the PAA, and the pH of PAA solutions was 6.0. Solutions with different counterions were obtained by adding an amount of base containing the anion needed for the measurement and fixing the pH at 9.0, respectively. All the PAA-*g*-PEO-7% solutions with different species of counterions (Na^+, K^+, and NH_4^+) were prepared at the desired polymer concentration (in the range from 10^{-2} to about 8.0 mg·mL^{-1} in order to completely cover the dilute and semidilute concentration). The DRS for each PAA and PAA-*g*-PEO-7% solution was measured directly after preparation, and some concentrations of PAA-*g*-PEO-7% solution were used for the temperature-dependent dielectric measurements.

2.2. Dielectric Measurement. Dielectric measurements (40 Hz to 110 MHz) were carried out with an impedance analyzer (Agilent Technology 4294A). The amplitude of the applied alternating field was 500 mV. The temperature of the sample was controlled by a circulating thermostated water jacket. The cell for dielectric measurements consists of concentrically cylindrical platinum electrodes.[36] The cell constant C_l and stray capacitance C_r determined by using two standard liquids (pure water, ethanol) and air were 0.477 and 0.109 pF, respectively. The value of the residual inductance L_r was determined by use of standard KCl solutions with different concentrations and the relation $C = L_rG^2$. Then, the values of capacitance C and conductance G measured directly were corrected for the residual inductance arising from the terminal leads and measurement cell according to the following equations:[37,38]

$$C_s = \frac{C_x(1 + \omega^2 L_r C_x) + L_r G_x^2}{(1 + \omega^2 L_r C_x)^2 + (\omega L_r G_x)^2} - C_r \quad (1)$$

$$G_s = \frac{G_x}{(1 + \omega^2 L_r C_x)^2 + (\omega L_r G_x)^2} \quad (2)$$

where the subscript x and s denote the directly measured and modified values, respectively, and ω ($\omega = 2\pi f$, f is measurement frequency) is the angular frequency. The equivalent circuit of the measuring cell is not listed here, and one can refer to the literature.[37,38] The corrected data of G and C at each frequency were converted to the corresponding dielectric permittivity ε and conductivity κ according to the following equations: $\varepsilon = C_s/C_l$

dx.doi.org/10.1021/jp2102379 |J. Phys. Chem. B 2012, 116, 763–774

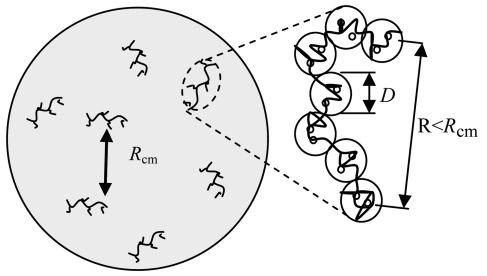

Figure 1. Polyelectrolyte chains in dilute solution. Empty circles on the chain are charged groups. The chains are self-avoiding walks of electrostatic blobs, and the size of the electrostatic blob is D. The chain size R is smaller than the distance R_{cm} between chains.

and $\kappa = G_s\varepsilon_0/C_l$ ($\varepsilon_0 = 8.8541\times 10^{-12}$ F/m is the vacuum permittivity).

3. REVIEW OF THE SCALING THEORY

As a common feature of most polyelectrolyte solutions, dielectric relaxations can be expected at low (around kHz), intermediate (between 1 and 100 MHz), and high (around GHz) frequency range.[39] The attribution of high-frequency relaxation is thought to be polarization of water molecules, but the mechanisms of low- and intermediate-frequency relaxations are still under controversy. Among present ideas to interpret the two relaxations, the scaling law proposed by Ito et al.[26] is extensively employed in recent investigations, which pointed out that the fluctuation of free counterions on the scale of a correlation length ξ gives rise to the intermediate relaxation. In addition, the polymer dynamics in solution can be well described by the Zimm dynamics model, which thought that the relaxation process can be viewed to be related to the hydrodynamic volume of the chain R^3.[27,40] However, two dielectric relaxations occur at the frequency range between 1 and 100 MHz in our case, and the relaxation mechanism of the two intermediate-frequency relaxations is unknown. In order to determine the relaxation mechanism and interpret our measuring result, it is necessary to briefly review the scaling approaches of Ito et al.[26] and Zimm dynamic model, using the notation of Dobrynin et al.,[27] to describe the intermediate-frequency relaxation dynamics of dilute and semidilute flexible polyelectrolyte aqueous solutions.

The polyelectrolyte solution contains charged flexible polyions built up of N (degree of polymerization) monomers (the size of monomer is b), each of them carrying an ionizable group of charge $|z_p|e$ and a counterion of charge $|z_p|e$, z_p and z_c being their valences, respectively. C_p is the polyelectrolyte concentration per unit volume. For the PAA and PAA-g-PEO solution in this study, $z_p = z_c = 1$. Owing to counterion condensation in a highly charged polyelectrolyte system,[41,42] a fraction of the counterions will condense on the polyions. After the condensation takes place, the counterions in polyelectrolyte solution are classified into two groups: condensed (or bound) and free counterions. If one sets f as the fraction of free counterions, $(1 - f)$ is the fraction of the condensed counterions.

3.1. Dilute Solution. In the dilute solution, the electrostatic screening length r_B ($r_B \approx (B/C_pb)^{1/2}$, where B is the ratio of the chain contour length Nb to the extended length L of chain) is smaller than the chain size R, and R is smaller than the distance R_{cm} between chains, as shown in Figure 1. The chain becomes flexible, so the polyions are self-avoiding walks of electrostatically screened blobs of size r_B, each of which is an extended configuration of electrostatic blobs of size D, as shown in Figure 1. The end-to-end distance R can be written as eq 4

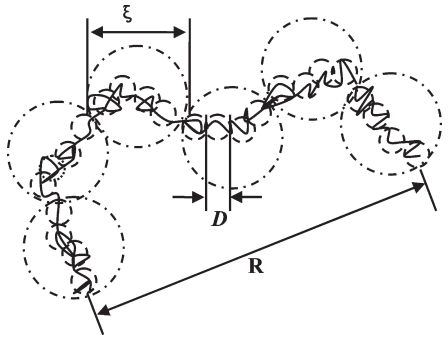

Figure 2. Polyelectrolyte chain in semidilute solution. The chain is a random walk of correlation blobs of size ξ, and the correlation blob is composed of several monomers of size D.

$$R_{cm} \approx (N/C_p)^{1/3} \tag{3}$$

$$R \approx b^{2/5}B^{-2/5}N^{3/5}C_p^{-1/5} \tag{4}$$

In dilute solution range, according to Ito et al.,[30,31] free counterions can polarize by 3D diffusion to a scale of the order of the distance between chains, R_{cm}, and the characteristic parameters of dielectric relaxation, the relaxation time τ, can be written as

$$\tau \approx \frac{R_{cm}^2}{2D_{ion}} \tag{5}$$

where D_{ion} is the diffusion coefficient of the counterions in solution. By substituting eq 3 into eq 5, we have

$$\tau \sim R_{cm}^2 \sim (C_p^{-1/3})^2 \propto C_p^{-2/3} \tag{6}$$

In addition, the polymer dynamics in this regime can be described by the Zimm dynamics model, and the relaxation time can be viewed as proportional to the hydrodynamic volume of the chain R^3, according to $\tau_{Zimm} \approx (\eta_s R^3)/(kT)$,[40,43] where η_s is the viscosity and kT is thermal energy. Considering R given by eq 4, the relaxation time in dilute solution can be given by

$$\tau \sim R^3 \sim (C_p^{-1/5})^3 \propto C_p^{-3/5} \tag{7}$$

The dielectric increment $\Delta\varepsilon$, which is proportional to the concentration of the polarized objects times the square of the dipole moment, reflects the polarization degree of polarized substance and can be given by

$$\Delta\varepsilon \approx n\mu^2 \approx fC_p\mu^2 \tag{8}$$

where n is the concentration of polarized objects, μ is the dipole moment, and fC_p is the concentration of the free counterions in polyelectrolyte solution.

In the dilute solution, according to Ito et al., free counterions can polarize within the distance R_{cm} between chains. By substituting eq 3 into eq 8, we have the dielectric increment $\Delta\varepsilon$

$$\Delta\varepsilon \approx n\mu^2 \approx fC_p\mu^2 \approx fC_p(eR_{cm})^2 \propto C_p^{1/3} \tag{9}$$

Moreover, the polymer dynamics can also be described by the Zimm dynamics model, which thought that R has effect on the

dx.doi.org/10.1021/jp2102379 |J. Phys. Chem. B 2012, 116, 763–774

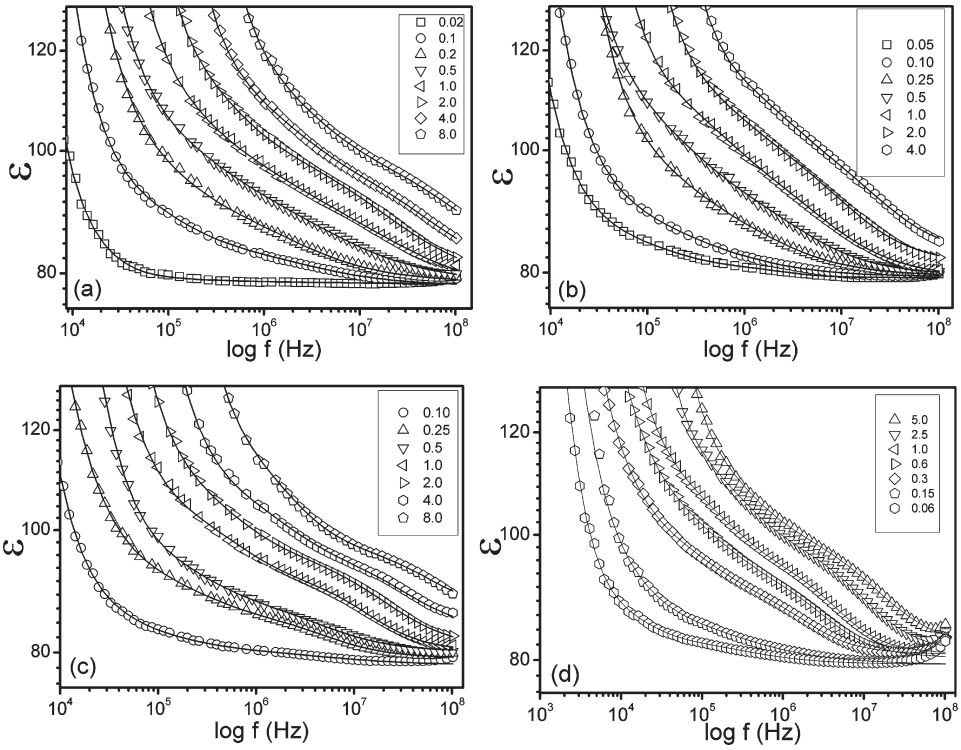

Figure 3. Dielectric spectra of PAA-*g*-PEO-7% solutions as a function of frequency, at a temperature of 25.0 °C and at a series of polymer concentrations (from 10^{-2} to about 8.0 mg·mL^{-1}), for different counterion species (a) K^+, (b) Na^+, and (c) NH_4^+. (d) Dielectric spectra of PAA solution at a concentration range from 10^{-2} to about 5.0 mg·mL^{-1}.

polymer dynamics. Considering R given by eq 4, the dielectric increment $\Delta\varepsilon$ in polyelectrolyte solution can be given by

$$\Delta\varepsilon \approx n\mu^2 \approx fC_p\mu^2 \approx fC_p(eR)^2 \propto C_p^{3/5} \quad (10)$$

3.2. Semidilute Solution. When the polyelectrolyte concentration is increased until the distance R_{cm} between chains equals their end-to-end length R, the polyelectrolyte concentration is just the overlap concentration C^*. At polyelectrolyte concentrations larger than C^*, the semidilute solution appears. The major feature of a semidilute solution ($C_p > C^*$) is the existence of the correlation length ξ as shown in Figure 2.[44] In this regime, electrostatic interactions are screened on a length scale which is larger than correlation length ξ ($\xi \approx (B/C_pb)^{1/2}$), and the chain is a random walk of correlation blobs of size ξ, each of which is composed of several monomers of size D, as illustrated in Figure 2.

In the semidilute solution ($C_p > C^*$), if Zimm dynamics model is applicable, the relaxation time is proportional to the cubic of the correlation length ξ^3 and can be expresses as[43]

$$\tau_{Zimm} \approx \frac{\eta_s\xi^3}{kT} \sim \xi^3 \sim (C_p^{-1/2})^3 \propto C_p^{-3/2} \quad (11)$$

According to Ito's model, the relaxation is caused by the free counterions polarization within the correlation lengthξin the semidilute solution. Therefore, the relaxation time can be written as

$$\tau \approx \frac{\xi^2}{2D_{ion}} \sim \xi^2 \sim (C_p^{-1/2})^2 \propto C_p^{-1} \quad (12)$$

Since both Ito's model and the Zimm dynamics model showed that the relaxations that occur at this semidilute regime are all connected to ξ, according to eq 8, the dielectric increment $\Delta\varepsilon$ in the semidilute solution is given by

$$\Delta\varepsilon \approx n\mu^2 \approx fC_p\mu^2 \approx fC_p(e\xi)^2 \propto C_p^0 \quad (13)$$

The above-stated dependences of the dielectric increment and the relaxation time on the polyelectrolyte concentration indicated that the dynamical processes such as ion fluctuations, chain motions, and the interaction are all influenced by conformation change of chains with the increase in polyelectrolyte concentration. The dynamics of the polyelectrolyte solution can be well described by either Ito's model or Zimm dynamics model. But which model is suitable for the present system will still need to be further verified by experiment. Therefore, in order to distinguish the intermediate-frequency relaxation mechanism, we will discuss our experimental results and compare our results with the above scaling theory.

4. RESULTS AND DISCUSSION

4.1. Dielectric Spectra of PAA-*g*-PEO-7% Solution of Different Concentrations. Figure 3 shows the dielectric spectra of PAA-*g*-PEO-7% and PAA aqueous solutions in a concentration range from 10^{-2} to about 8.0 mg·mL^{-1} at 25 °C, where panels a, b, and c show the frequency dependence of the permittivity of three PAA-*g*-PEO-7% solutions with three counterions, Na^+, K^+, and NH_4^+, respectively. From Figure 3, it can be seen that only one dielectric relaxation with a wide time distribution for each concentration can be observed at a frequency range about from10^6 to 10^8 Hz, and the relaxation shifts to higher frequency range with increasing concentration. Simultaneously, it is also obvious that the permittivity decreases sharply at a low frequency

dx.doi.org/10.1021/jp2102379 |*J. Phys. Chem. B* 2012, 116, 763–774

range and the location of the fall shifts to higher frequency with the increment in concentration. The remarkable falling phenomenon is recognized as a behavior caused by electrode polarization.

4.2. Determination of Dielectric Relaxation Parameters. In order to remove the effect of electrode polarization on the low-frequency relaxation, the Cole−Cole equation including two (i = 1, 2 for PAA solution) or three (i = 1, 2, 3 for PAA-g-PEO-7% solutions) Cole−Cole's terms combined with an electrode polarization term $A\omega^{-m}$ was employed:[45]

$$\varepsilon^* = \varepsilon_h + \sum_i \frac{\Delta\varepsilon_i}{1 + (j\omega\tau_i)^{\beta_i}} + A\omega^{-m} \quad (14)$$

where $\Delta\varepsilon_i$ ($=\varepsilon_{il} - \varepsilon_{ih}$) refers to the dielectric increment of the ith relaxation, ε_{il} and ε_{ih} are the low- and high-frequency limits of permittivity of the ith relaxation, respectively, $\tau_i = 1/2\pi f_{i0}$ (f_{i0} is the characteristic relaxation frequency) is the relaxation time of the ith relaxation, and β_i is the Cole−Cole parameter of the ith relaxation ($0 < \beta_i \leq 1$). A and m are adjustable parameters in the fitting process. i = 1, 2, 3, ... represent the relaxation from low to high frequency, respectively. In order to describe clearly, we replaced "1, 2, 3" with "l, m, h" to describe the $\Delta\varepsilon_i$, β_i, and τ_i in the following discussion. After the parameters A and m are determined by fitting eq 14 to the raw data of real part of permittivity, the electrode polarization term $A\omega^{-m}$ can be subtracted from the raw date and the corrected real part of permittivity can be obtained.

The measured total dielectric loss $\kappa/\varepsilon_0\omega$ contain the contribution due to the dielectric loss ε'' and the dc conductivity contribution $\kappa_l/\varepsilon_0\omega$. Considering the high dc electrical conductivity of our system, the $\kappa_l/\varepsilon_0\omega$ term should not be neglected. Therefore, the dielectric loss ε'' should be calculated with eq 15, in which the contribution of dc electrical conductivity was subtracted.[39]

$$\varepsilon'' = \frac{\kappa - \kappa_l}{\omega\varepsilon_0} \quad (15)$$

where the stable value of the dc term, κ_l, was directly read out from the conductivity spectra.

After the effect of electrode polarization and the contribution of dc electrical conductivity were removed from the real and imaginary part of permittivity, respectively, the dielectric relaxation parameters were obtained by simultaneously fitting the Cole−Cole equation to the corrected real and imaginary part of the dielectric spectra and are listed in Tables 1 and 2.

As an example of the best-fitting curves by the Cole−Cole equation, typical results for PAA and PAA-g-PEO-7% aqueous solutions are shown in Figure 4a,b for two different polyelectrolyte solutions at similar concentrations. Figure 4, a and b,

Table 1. Dielectric Parameters of PAA Solutions (pH = 6.0) with Different Concentrations Obtained by Fitting the Dielectric Spectra

C_p(mg/mL)	β_l	β_h	$\Delta\varepsilon_l$	$\Delta\varepsilon_h$	τ_l/s	τ_h/s
5	0.76	0.75	18.72	17.15	4.64×10^{-7}	1.11×10^{-8}
2.5	0.80	0.81	18.19	15.93	4.94×10^{-7}	1.66×10^{-8}
1.0	0.71	0.89	19.35	11.29	8.08×10^{-7}	3.53×10^{-8}
0.6	0.60	0.91	20.67	7.62	9.92×10^{-7}	4.30×10^{-8}
0.3	0.65	0.91	14.81	6.00	1.19×10^{-6}	7.11×10^{-8}
0.15	1.00	0.59	3.01	8.54	6.70×10^{-6}	7.20×10^{-7}
0.06	1.00	0.69	3.17	3.78	6.62×10^{-6}	4.80×10^{-7}

Table 2. Dielectric Parameters of Different Concentrations of PAA-g-PEO-7% Solutions Obtained by Fitting: (A) K^+ as a Counterion, pH = 9.0; (B) Na^+ as a Counterion, pH = 9.0; and (C) NH_4^+ as a Counterion, pH = 9.0

C_p(mg/mL)	β_l	β_m	β_h	$\Delta\varepsilon_l$	$\Delta\varepsilon_m$	$\Delta\varepsilon_h$	τ_l/s	τ_m/s	τ_h/s
(A) K^+ as a Counterion, pH = 9.0									
0.1	0.76	0.80	0.70	13.49	7.26	4.76	1.12×10^{-5}	1.08×10^{-6}	4.51×10^{-8}
0.2	0.76	0.71	0.59	33.53	14.60	10.17	1.75×10^{-5}	1.53×10^{-6}	3.82×10^{-8}
0.5	0.81	0.75	0.73	33.89	14.67	9.74	8.32×10^{-6}	3.67×10^{-7}	1.44×10^{-8}
1.0	0.83	0.74	0.58	14.84	8.36	17.38	1.06×10^{-6}	1.59×10^{-7}	9.70×10^{-9}
2.0	0.80	0.83	0.49	15.59	2.15	33.03	3.64×10^{-7}	3.91×10^{-8}	2.80×10^{-9}
4.0	0.70	0.75	0.45	32.41	8.29	33.28	1.30×10^{-6}	6.56×10^{-8}	1.10×10^{-9}
8.0	0.70	0.55	0.89	24.41	28.29	5.89	7.96×10^{-7}	3.18×10^{-8}	$4.08 \times 10^{-1}0$
(B) Na^+ as a Counterion, pH = 9.0									
0.05	0.77	0.84	0.76	13.50	2.96	1.88	1.28×10^{-5}	8.50×10^{-7}	1.27×10^{-7}
0.10	0.73	0.86	0.72	22.98	2.87	3.86	9.45×10^{-6}	5.83×10^{-7}	1.28×10^{-7}
0.25	0.73	0.86	0.72	22.22	5.29	9.69	4.58×10^{-6}	4.98×10^{-7}	8.52×10^{-8}
0.5	0.76	0.86	0.74	22.91	9.23	13.53	3.64×10^{-6}	4.87×10^{-7}	4.84×10^{-8}
1.0	0.76	0.84	0.74	20.96	13.04	17.07	4.80×10^{-6}	2.59×10^{-7}	2.60×10^{-8}
2.0	0.62	0.75	0.80	26.91	11.67	15.35	3.13×10^{-6}	1.27×10^{-7}	1.45×10^{-8}
(C) NH_4^+ as a Counterion, pH = 9.0									
0.10	0.71	0.73	0.69	15.66	3.03	1.79	1.84×10^{-5}	1.27×10^{-6}	2.49×10^{-8}
0.25	0.94	0.71	0.87	14.70	10.63	4.90	7.43×10^{-6}	7.12×10^{-7}	2.76×10^{-8}
0.5	0.93	0.74	0.81	25.12	11.10	5.97	7.69×10^{-6}	5.84×10^{-7}	2.85×10^{-8}
1.0	0.82	0.88	0.87	27.35	10.12	10.88	3.79×10^{-6}	2.18×10^{-7}	1.15×10^{-8}
2.0	0.84	0.86	0.78	19.45	11.08	14.82	1.96×10^{-6}	2.29×10^{-7}	8.15×10^{-9}
4.0	0.84	0.86	0.83	25.24	11.17	11.15	1.13×10^{-6}	7.30×10^{-8}	4.59×10^{-9}
8.0	0.84	0.86	0.89	12.08	19.46	9.14	8.34×10^{-7}	7.30×10^{-8}	2.62×10^{-9}

dx.doi.org/10.1021/jp2102379 |J. Phys. Chem. B 2012, 116, 763–774

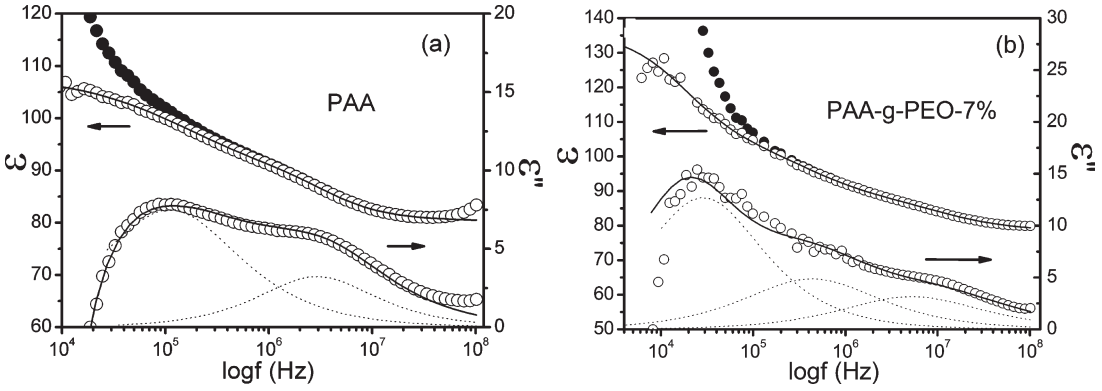

Figure 4. At 25.0 °C, the dielectric permittivity, ε, and loss data, ε'', of (a) a PAA solution with $C_p = 0.6$ mg·mL^{-1} and (b) a PAA-*g*-PEO-7% solution with $C_p = 0.5$ mg·mL^{-1} as a function of frequency. ● represents the original data, ○ represents the calculated data. The solid lines are the best-fit curve with the Cole−Cole equation. The dashed lines are the fitted result for each relaxation.

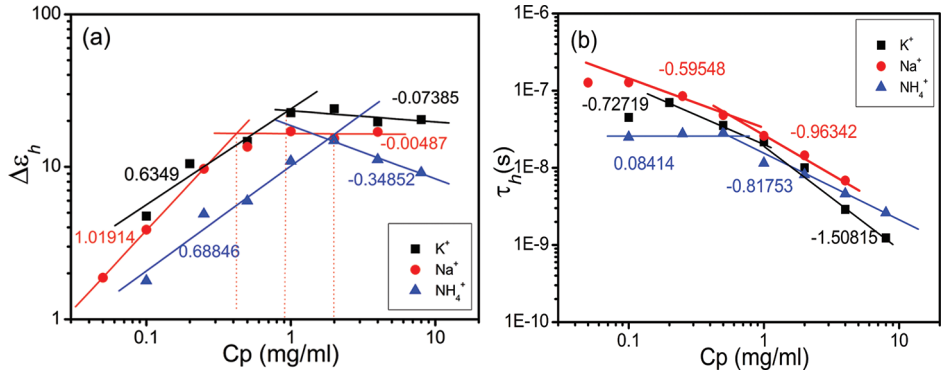

Figure 5. Dependences of the high-frequency characteristic parameters (a) the dielectric dispersion $\Delta\varepsilon_h$ and (b) the relaxation time τ_h of PAA-*g*-PEO-7% solution with Na^+, K^+, and NH_4^+ as counterions on the polyelectrolyte concentration C_p.

respectively, shows the frequency dependence of the permittivity ε and dielectric loss ε'' of PAA solution ($C_p = 0.6$ mg·mL^{-1}) and PAA-*g*-PEO-7% solution ($C_p = 0.5$ mg·mL^{-1}) with K^+ as a counterion at 25 °C. It should be noted that in Figure 4a,b the permittivity curves indicated by open circles are the processed data whose electrode polarization effect at low-frequency has been eliminated from the original data (showed in the solid circle) by the method in the literature.[46] The dielectric loss curves obtained by eq 15 are also shown in open circles and the solid lines are the fitting results with the Cole−Cole equation. It also can be seen from Figure 4 that the maximum of ε'' as a function of frequency clearly evidences the number of dielectric dispersions in the frequency range investigated. It is noticeable that the dielectric spectroscopy of the PAA solution shows two relaxations (Figure 4a) and the dielectric spectroscopy of PAA-*g*-PEO-7% solution shows three relaxations (Figure 4b). The more relaxations can be considered to be in connection with the grafted PEO.

4.3. Dielectric Relaxation Mechanism of PAA-*g*-PEO-7% Solution. *4.3.1. High-Frequency Relaxation.* In order to study the relaxation mechanism, the high-frequency dielectric increment $\Delta\varepsilon_h$ and relaxation time τ_h, in the presence of three types of counterions (Na^+, K^+, and NH_4^+), in Table 2 were plotted as a function of the PAA-*g*-PEO-7% concentration C_p in Figure 5, a and b, respectively. Figure 5a shows that the $\Delta\varepsilon_h$ of PAA-*g*-PEO-7% solutions with three types of counterions are all proportional to the concentration in dilute solution and nearly unchanged in semidilute solution for Na^+ and K^+. From Figure 5b, it can be seen that the values of high-frequency relaxation time τ_h are mainly in the order $\tau_{Na^+} > \tau_{K^+} \geq \tau_{NH_4^+}$ for the same concentration in this experiment. If we assume that the observed high-frequency relaxation should be attributed to the fluctuation of the free counterions, the relaxation time would be inversely proportional to the ion diffusion coefficient D_{ion} according to eqs 5 and 12. The values of D_{ion} for Na^+, K^+, and NH_4^+ are $D_{Na^+} = 1.334 \times 10^{-5}$ cm^2 s^{-1}, $D_{K^+} = 1.957 \times 10^{-5}$ cm^2·s^{-1}, and $D_{NH_4^+} = 1.957 \times 10^{-5}$ cm^2·s^{-1}.[47] But when the significant digit increases, we thought that the values of diffusivity for K^+ and NH_4^+ are not exactly the same, and consequently the order of D_{ion} is $D_{NH_4^+} \approx D_{K^+} > D_{N_{a+}}$. According to eqs 5 and 12, the order of the high-frequency relaxation time τ_h should be $\tau_{Na^+} > \tau_{K^+} \approx \tau_{NH_4^+}$. But in the literature,[48] the order of relaxation time for the free ions was reported as follows: $\tau_{Na^+} > \tau_{K^+} > \tau_{NH_4^+}$. Therefore, we thought that the order of the high-frequency relaxation time τ_h should be $\tau_{Na^+} > \tau_{K^+} \geq \tau_{NH_4^+}$, which is in good agreement with our experimental result in Figure 5b. This good agreement gives support to the hypothesis that the high-frequency relaxation originates from the fluctuation of free counterions.

As can be seen from Figure 5, the relaxation time and the dielectric increment undergo a good scaling behavior with well-defined scaling exponents in either the dilute or semidilute

dx.doi.org/10.1021/jp2102379 |*J. Phys. Chem. B* 2012, 116, 763–774

Table 3. Scaling Indices m and n in the Concentration Dependence of the Dielectric Parameters $\Delta\varepsilon$ (Index q) and τ (Index n) of PAA-*g*-PEO-7% Aqueous Solutions

				expl values (different counterions)		
dielectric parameters	polyelectrolyte concn	expected values		K^+	Na^+	NH_4^+
dielectric increment	dilute solution	3/5	eq 10, Zimm	0.63		0.69
$\Delta\varepsilon \approx C_p^q$				1.02		
		1/3	eq 9, Ito			
	semidilute solution	0	eq 13, Zimm, Ito	−0.07	−0.005	−0.35
relaxation time	dilute solution	−2/3	eq 6, Ito	−0.73		
$\tau \approx C_p^n$		−3/5	eq 7, Zimm		−0.60	
						0.084
	semidilute solution	−3/2	eq 11, Zimm	−1.51		
		−1	eq 12, Ito		−0.96	
						−0.81753

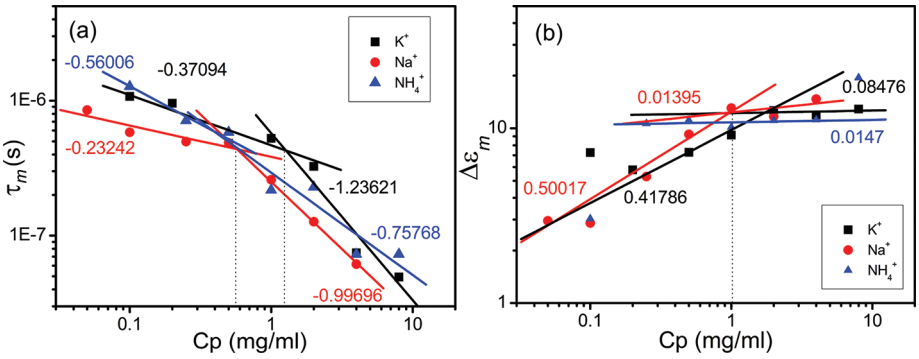

Figure 6. Dependences of (a) the relaxation time τ_m and (b) the dielectric increment $\Delta\varepsilon_m$ of PAA-*g*-PEO-7% solution on the concentration C_p, for Na^+, K^+, and NH_4^+.

solution. The experimental values and those expected on the basis of the scaling laws eq 6 −13 are collected in Table 3.

In Figure 5a and Table 3, it is obvious that the slopes of curves for counterions K^+ and NH_4^+ in dilute solution are 0.63 and 0.69, respectively, being not too far from the values expected from eq 10, $\Delta\varepsilon \propto C_p^{3/5}$. This shows that the scaling of the dielectric increment in the dilute solution is consistent with the expectation of Zimm dynamics. On the other hand, in the semidilute solution, the dielectric increment scales with an index −0.07 for K^+ and −0.005 for Na^+, all being consistent with the expected independence of the polymer concentration $\Delta\varepsilon \propto C_p^0$ (eq 13), which was derived from the Zimm dynamics and Ito's model. Therefore, in the whole concentration range, the scaling behavior of the dielectric increment is in good agreement with the prediction by Zimm dynamics, suggesting that end-to-end distance R of the chain in the dilute solution and the correlation length ξ in a semidilute solution have effect on the polyelectrolyte dynamics.

From Figure 5b and Table 3, we can also see that the relaxation time in the dilute solution scales with an index −0.60 for PAA-*g*-PEO-7% solution with Na^+ as a counterion, in good agreement with the prediction by Zimm dynamics $\tau \propto C_p^{-3/5}$ (eq 7). In the semidilute solution, the scaling behavior described by $\tau \propto C_p^{-1.51}$ for the K^+ is consistent with the expectation of Zimm dynamics $\tau \propto C_p^{-3/2}$ (eq 11). In addition, we observe scaling laws $\tau \propto C_p^{-0.73}$ for PAA-*g*-PEO-7% solution with K^+ as a counterion in the dilute solution, which seems to be not close to eq 6, $\tau \propto C_p^{-2/3}$ (Ito's model). And the scaling of the relaxation time for Na^+ can be described by $\tau \propto C_p^{-0.96}$ in the semidilute solution, which is a little far from eq 12, $\tau \propto C_p^{-1}$ (Ito's model). Compared to Ito's model and Zimm dynamics model, we thought that the scaling of the relaxation time is numerically in reasonable agreement with the scaling behavior of the Zimm dynamics in the whole concentration range. This suggested that the dynamic processes in polyelectrolyte solution depend on the hydrodynamic volume of the chain R^3 in the dilute solution and the cubic of the correlation length ξ^3 in the semidilute solution.

Finally, it was proved by the relaxation time of different counterions that the high-frequency relaxation originates from the fluctuation of the free counterions. Considering the scaling of both the dielectric increment and the relaxation time with the concentration in the dilute and semidilute solution, the scaling behaviors are numerically more close to that predicted by Zimm dynamics. It means that the free counterions is fluctuating along the chain end-to-end distance R as shown in Figure 1 in a dilute solution, and has the polarization in the correlation length ξ range in a semidilute solution, as shown in Figure 2.

4.3.2. Middle-Frequency Relaxation. Figure 6, a and b, shows the dependences of the relaxation time τ_m and dielectric increment $\Delta\varepsilon_m$ of middle-frequency for PAA-*g*-PEO-7% solutions with different counterions (Na^+, K^+, and NH_4^+) on the polyelectrolyte concentration C_p, respectively. It can be seen from Figure 6a that the order of the middle-frequency relaxation time τ_m for the same concentration is $\tau_{Na^+} < \tau_{K^+} \leq \tau_{NH_4^+}$, which is

dx.doi.org/10.1021/jp2102379 |J. Phys. Chem. B 2012, 116, 763–774

different from that of the high-frequency relaxation time ($\tau_{Na^+} > \tau_{K^+} \geq \tau_{NH_4^+}$). Therefore, the middle-frequency relaxation should not be attributed to the fluctuation of free counterions. From Figure 6b, it can be seen that the dielectric increment $\Delta\varepsilon_m$ for the three types of counterions all undergo scaling behaviors with the C_p in the whole concentration range, which indicates that the relaxation is due to the fluctuation of the condensed counterions, since the high-frequency relaxation is due to free counterions as the discussion above in section 4.3.1. In addition, the values of $\Delta\varepsilon_m$ and the change of the mid- frequency dielectric increment with C_p are similar to that reported by Mandel.[49] This suggests that the mid-frequency relaxation occurring at the frequency range of 100 kHz to 5 MHz should be attributed to the polarization caused by the fluctuation of the condensed counterions.[30,31]

In our results, the relaxation process caused by the fluctuation of the condensed counterions exits at about megahertz, whereas this relaxation process ought to appear at around the kilohertz frequency range according to the reports from Ito et al.[30,31] This difference in relaxation frequency between Ito's work and ours may be partly due to the molecular structure of PAA-*g*-PEO. The side-chain PEOs divided the main chain PAA into several parts and the fluctuation of the condensed counterions along the whole polyelectrolyte chain was restricted in a shorter distance. As a result, the relaxation frequency shifted from kilohertz to a higher frequency, megahertz.

From Figure 6a,b, the scaling behavior of the relaxation time τ_m and the dielectric increment $\Delta\varepsilon_m$ as a function of concentration were obtained. As can be seen from Figure 6b, the scaling behavior of $\Delta\varepsilon_m$ can be described by $\Delta\varepsilon_m \propto C_p^{1/2}$ for Na^+, and the scaling index are 0.42 for K^+ in dilute solution. Unfortunately, the scaling value for NH_4^+ in the dilute solution was not obtained from the experiment for lack of data. Unlike dilute solution, in the semidilute solution, the dielectric increment $\Delta\varepsilon_m$ for the three types of counterions shows the same scaling behavior ($\Delta\varepsilon_m \propto C_p^0$). In other words, the values of $\Delta\varepsilon_m$ for all the three types of counterions increase with rising C_p in dilute solution, while the corresponding values are nearly unchanged in the semidilute solution, as shown in Figure 6b. With respect to the relaxation time τ_m, the scaling behavior of τ_m in dilute solution can be respectively described by $\tau_m \propto C_p^{-0.37}$ (for K^+), $\tau_m \propto C_p^{-0.23}$ (for Na^+), $\tau_m \propto C_p^{-0.56}$ (for NH_4^+) and the value of scaling index in semidilute solution varies between the three different counterions: −1.23 for K^+, −1.00 for Na^+, and −0.76 for NH_4^+. The obtained scaling indexes are different for the three kinds of counterions, but the change of these scaling index with the concentration C_p has the same tendency in either dilute or semidilute solution, as can be seen from Figure 6a. This suggests that the relaxation is due to the condensed counterion. Because it is difficult to analyze the relaxation caused by the condensed counterion, which is often covered by electrode polarization effect, the real scaling laws of the relaxation for the polyelectrolyte solution are not still determined. Therefore, we cannot compare our experimental results with the expected scaling laws as the analysis of high-frequency relaxation. It should be pointed out that the above obtained scaling index of middle-frequency relaxation may be only for grafted PAA-*g*-PEO solution system in our case. Further study is necessary to determine whether or not the scaling index is suitable for the other polyelectrolyte or grafted polyelectrolyte.

4.3.3. Low-Frequency Relaxation. With regard to the low-frequency relaxation, the scaling approach is inapplicable to determine the relaxation mechanism. In addition, although polyelectrolyte solution has been extensively investigated by DRS, there has been less research on low-frequency relaxation. This is because the relaxation is often covered by electrode polarization effect and cannot be observed as stated above. Fortunately, this effect has been eliminated from the dielectric data in this work in the way described in the literature[46] (see Figure 4b), and the dielectric parameters of the low-frequency relaxation were obtained as listed in Table 2. The following discussion was focused on how the relaxation occurs.

It can be seen from Table 2 that the change of dielectric increment is relevant with ion species. The $\Delta\varepsilon_l$ for PAA-*g*-PEO-7% solution with Na^+ as a counterion is constant with rising C_p in the dilute solution, and increases with the rise of C_p in the semidilute solution. But, for PAA-*g*-PEO-7% solution with K^+, and NH_4^+ as counterions, the $\Delta\varepsilon_l$ increase in the dilute solution and decrease in the semidilute solution. It is also obvious in Table 2 that the relaxation time τ_l is also relevant with ion species. The τ_l for PAA-*g*-PEO-7% solution with K^+ decreases slowly with rising C_p in the dilute solution and decreases faster with the rise of C_p in the semidilute solution, whereas for the PAA-*g*-PEO-7% solution with Na^+ and NH_4^+, the relaxation time decreases quickly in the dilute solution and slowly in the semidilute solution. Therefore, it can be concluded that the low-frequency relaxation is related to ion species.

From the above discussion, it is clear that, only from the change of $\Delta\varepsilon_l$ and τ_l in Table 2 with the C_p, we cannot judge polarization mechanism. According to the molecular structure of PAA-*g*-PEO-7%, ether oxygen atoms in grafted side-chain PEO which have lone-electron pair have a strong affinity to the electronic acceptor, that is, the carboxyl carbon of PAA (pH = 9.0, PAA completely ionization). In addition, the results from light scattering showed that the hydrogen bonding between carboxylic group and ether oxygen led to the formation of large complexes among PAA-*g*-PEO chains.[24] The above fact indicated that the large complex indeed formed through the hydrogen-bonding interaction between the grafted side-chain PEO and the PAA backbone. In addition, compared to the dielectric spectra of PAA solution, the number of relaxations for the PAA-*g*-PEO-7% solution is one more than that for PAA solution, which shows that the new relaxation for the PAA-*g*-PEO-7% solution should be associated with the grafted side-chain PEO which formed the large complex. On the other hand, the value of the $\Delta\varepsilon_l$ for PAA-*g*-PEO-7% solution with Na^+, K^+, and NH_4^+ as counterions is about between 10 and 34, which is greater than the $\Delta\varepsilon_m$ ($\leq$10). According to our experience, the dielectric increment of interface polarization is usually big, so we thought the relaxation mechanism is due to the interface polarization. Finally, taking the above factors into consideration, we thought that the low-frequency relaxation can be attributed to interface polarization between the complex, which can be considered as a microsphere,[50] and the aqueous solution phase.

For the sake of argument, the possible microstructure of PAA-*g*-PEO molecule in dilute and semidilute solution is schematically illustrated in Figure 7. The complex in Figure 7 can be regarded as spherical particle, and the circular area indicated by broken lines represents a dispersion composed of the complex particle and aqueous medium. According to the following Hanai's equation (eq 16),[51,52] the volume fractions of the complex in various PAA-*g*-PEO-7% solutions were calculated.

$$\frac{\varepsilon_h - \varepsilon_j}{\varepsilon_a - \varepsilon_j}\left(\frac{\varepsilon_a}{\varepsilon_h}\right)^{1/3} = 1 - \phi \qquad (16)$$

where ϕ is the volume fraction of the disperse phase (complex in this case) and the subscripts a and j denote the continuous medium and the dispersed particles, respectively.

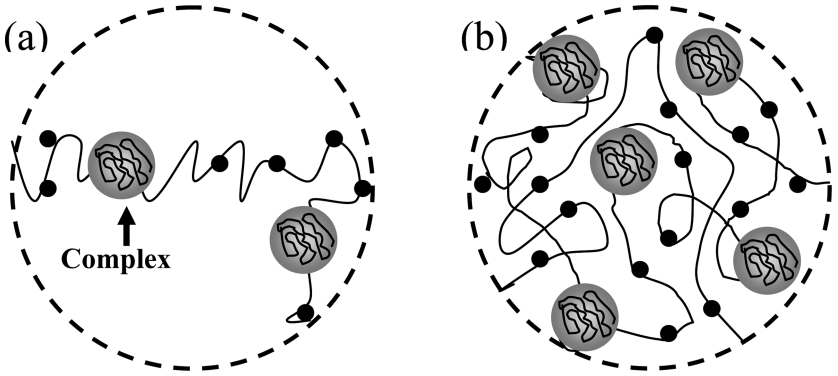

Figure 7. Schematic illustration of possible configuration and microstructure of PAA-*g*-PEO-7% molecules (a) in a dilute solution and (b) in a semidilute solution. The dots and the balls represent the fixed charges on the chains and the complex, respectively.

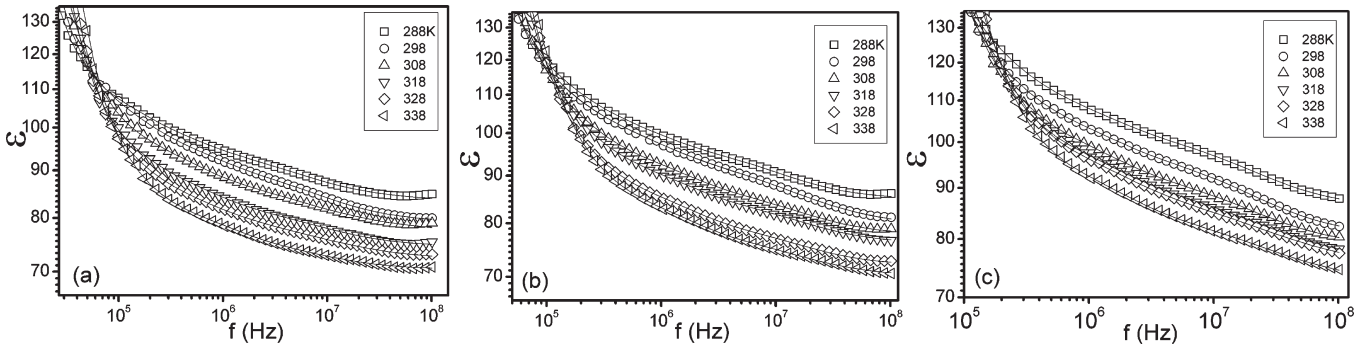

Figure 8. Frequency dependences of permittivity of PAA-*g*-PEO-7% solutions with K^+ as a counterion at three concentrations, (a) C_p = 0.5 mg·mL^{-1}, (b) C_p = 1.0 mg·mL^{-1}, and (c) C_p = 2.0 mg·mL^{-1}, at a series of temperature (from 288 to 338 K).

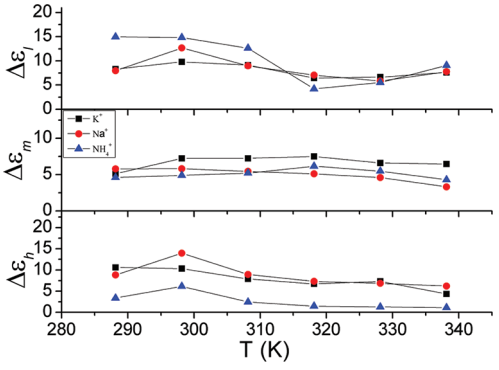

Figure 9. Low-, mid-, and high-frequency dielectric increment ($\Delta\varepsilon_l$, $\Delta\varepsilon_m$, $\Delta\varepsilon_h$) of PAA-*g*-PEO-7% solutions for three counterion species, K^+, Na^+, NH_4^+, as a function of temperature *T*.

The calculated results show that the value of ϕ is about 21.3−29.2% when the concentration of the PAA-*g*-PEO-7% solution is between 0.5 and 2 mg·mL^{-1}. According to the literature,[24] each PAA molecule grafted around 9.4 PEO molecules in PAA-*g*-PEO-7% molecules. In other words, the concentration of the complex formed by the side-chain PEO is greater than the PAA-*g*-PEO-7% concentration. Therefore, the large value (21.3−29.2%) of ϕ is reasonable. This result suggests that the grafted long side-chain PEO is inclined to forming complex with main-chain PAA, not like the charged short side-chain which can fluctuate or polarize in the field.[12,13] In conclusion, we thought that the low-frequency relaxation originates from the interface polarization effect between the complex and aqueous solution.

4.4. Dielectric Spectra of PAA-*g*-PEO-7% Solution at Different Temperatures. Figure 8 shows the dielectric spectra of PAA-*g*-PEO-7% solutions with K^+ as a counterion at three different concentrations, which were measured at a series of temperatures. The dielectric spectra of PAA-*g*-PEO-7% solution with Na^+ and NH_4^+ are omitted because they are similar to that of K^+. The dielectric parameters, dielectric increment and relaxation time, for PAA-*g*-PEO-7% solution with K^+, Na^+, and NH_4^+ at C_p = 0.5 mg·mL^{-1} were obtained from their dielectric spectra according to the method described in section 4.2.

For clarity, the dielectric increments ($\Delta\varepsilon_l$, $\Delta\varepsilon_m$, $\Delta\varepsilon_h$) at low-, mid-, and high-frequency range for three counterions K^+, Na^+, and NH_4^+ were plotted against measuring temperature *T* as shown in Figure 9.

As can be seen from Figure 9, the mid-frequency dielectric increment $\Delta\varepsilon_m$ has a small change with the rise of *T*, and the low- and high-frequency dielectric increments $\Delta\varepsilon_l$ and $\Delta\varepsilon_h$ slightly decrease with the rising temperature. The change of $\Delta\varepsilon_l$ is explained as follows. The low-frequency relaxation originates from interface polarization of the complex, which is formed through the hydrogen bonding between the carboxylic group of PAA and ether oxygen on the side-chain PEO. The rise of *T* can weaken hydrogen bonding,[53] resulting in the decrease of the complex. Therefore, the $\Delta\varepsilon_l$ changes with the rising temperature. For the high frequency, the relaxation mechanism is due to the

dx.doi.org/10.1021/jp2102379 |*J. Phys. Chem. B* 2012, 116, 763–774

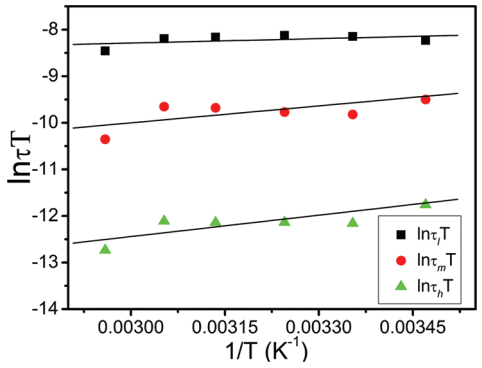

Figure 10. ln $\tau_l T$, ln $\tau_m T$, and ln $\tau_h T$ of PAA-*g*-PEO-7% solution with K^+ as a counterion, at C_p = 0.5 mg·mL^{-1}, as a function of $1/T$.

fluctuation of free counterions. According to eq 8 ($\Delta\varepsilon \approx n\mu^2 \approx fC_p\mu^2$), when the polyelectrolyte concentration C_p is fixed, the fraction f of free counterions increases with the rise of T,[54] and so the decrease of $\Delta\varepsilon_h$ can be attributed to the fact that the fluctuation range of free counterions decreases with the rise of T. From Figure 9, it is obvious that $\Delta\varepsilon_m$ was almost independent of ion species, suggesting that the mid-frequency relaxation originates from the polarization of condensed counterions. We can also see from Figure 9 that the $\Delta\varepsilon_h$ is dependent on ion species, which implied that the high-frequency relaxation is due to the fluctuation of free counterions, the same as the result in section 4.3.1.

The relaxation time obtained from the dielectric spectra reflects the internal dynamics information of the investigated system. Considering the relationship of the macro relaxation time and the relaxation rate constant τ (=1/k), the Eyring equation can be expressed as[55]

$$\ln \tau = \ln\left(\frac{h}{kT}\right) - \frac{\Delta S}{R} + \frac{\Delta H}{RT} \quad (17)$$

where h is Planck's constant and ΔH and ΔS are activation enthalpy and activation entropy of the relaxation process, respectively. In order to obtain ΔH and ΔS, the eq 17 was deformed to

$$\ln \tau T = \ln\left(\frac{h}{k}\right) - \frac{\Delta S}{R} + \frac{\Delta H}{RT} \quad (18)$$

According to eq 18, a plot of the function ln τT vs $1/T$ should give a straight line in which the slope and the intercept are related to the enthalpy ΔH and entropy ΔS, respectively. The ln $\tau_l T$, ln $\tau_m T$, and ln $\tau_h T$ were plotted as a function of $1/T$ for all the concentrations of PAA-*g*-PEO-7% solutions with different counterion species. Figure 10 gives an example of C_p = 0.5 mg·mL^{-1}, one of the PAA-*g*-PEO-7% solutions with K^+ ion. According to eq 18, the low-, mid-, and high-frequency ΔH and ΔS for PAA-*g*-PEO-7% solutions with the same C_p = 0.5 mg·mL^{-1} but different counterions and with the same K^+ ion but different concentrations were calculated and the results are listed in Table 4.

Table 4A shows the thermodynamic parameters of the low, mid, and high frequency of PAA-*g*-PEO-7% solutions with different counterions at C_p = 0.5 mg·mL^{-1}. As can be seen, all the entropy ΔS for different counterions are below 0. It may not be too pedantic to underline the fact that it is actually the entropy term that destabilizes the ordered, charged structure. Therefore,

Table 4. Thermodynamic Parameters for the PAA-*g*-PEO-7% Solutions with (A) the Same C_p = 0.5 mg·mL^{-1} but Different Counterions and (B) the Same K^+ Ion but Different Concentrations, Obtained by the Eyring Equation

(A) Same C_p = 0.5 mg·mL^{-1} but Different Counterions

thermodynamic parameters for different counterions		low freq	mid freq	high freq
ΔH (kJ·mol^{-1})	K^+	2.63	10.09	12.74
	Na^+	1.06	−5.03	−3.17
	NH_4^+	9.31	−7.68	−4.22
ΔS (J·K^{-1}·mol^{-1})	K^+	−120.76	−84.14	−55.87
	Na^+	−127.58	−138.10	−114.68
	NH_4^+	−105.28	−143.00	−110.50

(B) Same K^+ Ion but Different Concentrations

C_p(mg·mL^{-1})	ΔS_l	ΔH_l	ΔS_m	ΔH_m	ΔS_h	ΔH_h
0.5	−120.76	2627.44	−84.14	10085.66	−55.87	12740.45
1.0	−124.14	1051.45	−89.22	7001.86	−78.96	4064.62
2.0	−137.43	−3259.76	−109.13	398.90	−83.96	1582.99

the ΔS < 0 suggested that the low-, mid-, and high-frequency processes all undergo the intramolecular conformational transition of the PAA-*g*-PEO-7% from the disordered form to the fundamental ordered conformation. As far as the enthalpy change is concerned, the results in Table 4A clearly show that specific effects between the different counterions are not very small. This is not surprising if one takes into account the conformations involved in the transition from disordered form to ordered conformation. In our conditions, there should be the same electrostatic interactions between the polyelectrolyte and different counterions, because the PAA-*g*-PEO-7% solutions with different counterions have the same pH. Therefore, this difference of the enthalpy change between the different counterions can be most reasonably explained in terms of a generalized effect on the structure of the solvent, brought about by the individual characteristics of counterions (e.g., hydration, ionic radius) .

Table 4B shows the thermodynamic parameters of the low, mid, and high frequency of PAA-*g*-PEO-7% solution with K^+ ion at different concentrations (0.5, 1.0, and 2.0 mg·mL^{-1}). As can be seen, the enthalpy change of the three relaxation processes shows a general tendency to decrease with the rising concentration for the three concentrations investigated. This can be explained as follows: with increasing concentration, the blob size (D in Figure 1) decreases as a consequence of the deformation of PAA-*g*-PEO-7% chains, and hence the enthalpy change decreases.[56] This suggested that the energy needed by the low-, mid-, and high-frequency relaxation processes to overcome the obstacles decreases with increasing concentration. Considering that the low-frequency relaxation is due to interface polarization, the decrease of energy with concentration suggested the complex becomes smaller due to the conformation change of the macromolecule with the rising concentration. For the mid- and high-frequency relaxation process, the decrease of enthalpy can be explained as the fluctuations range of the condensed or free counterions decreases because of the conformation change of the macromolecule. Table 4B also shows that all the entropy change ΔS for the three concentrations investigated are below 0. Generally speaking, the low-, mid-, and high-frequency processes

dx.doi.org/10.1021/jp2102379 |*J. Phys. Chem. B* 2012, 116, 763–774

all undergo the conformational change of the PAA-*g*-PEO-7% from disordered form to ordered conformation.

5. CONCLUSION

The dielectric behaviors of PAA and PAA-*g*-PEO-7% in aqueous solution have been investigated over a frequency range of 40 Hz to 110 MHz at different concentrations and temperatures. After the contribution of electrode polarization was successfully subtracted, the dielectric spectra of PAA-*g*-PEO-7% solutions showed three relaxation processes in the experimental frequency range, which is one more relaxation than for the PAA solution. The observed three dielectric relaxations were strictly analyzed by Cole−Cole function and the dielectric parameters were obtained.

The three relaxations of PAA-*g*-PEO solution were discussed separately by the obtained dielectric parameters. Using different counterions species, it was proved that the high-frequency relaxation originates from the fluctuation of free counterions. In addition, the dependences of characteristic parameters, dielectric dispersion $\Delta\varepsilon$ and relaxation time τ, on the polyelectrolyte concentration C_p were discussed and compared with the predictions of scaling theories. The results showed that, in the dilute solution, the scaling of the dielectric increment for K^+ and NH_4^+ was more consistent with the expectation of Zimm dynamics $\Delta\varepsilon \propto C_p^{3/5}$ (eq 10). And in the semidilute solution, the scaling of $\Delta\varepsilon$ for K^+ and Na^+ agrees with the expected independence of the polymer concentration $\Delta\varepsilon \propto C_p^{0}$ (eq 13). As for relaxation time, we observed scaling laws $\tau \propto C_p^{-0.59}$ for Na^+ in the dilute solution and $\tau \propto C_p^{-1.51}$ for the K^+ in the semidilute solution, which were in good agreement with Zimm dynamics model $\tau \propto C_p^{-3/5}$ (eq 7) and $\tau \propto C_p^{-3/2}$ (eq 11), respectively. Considering the scaling of both the dielectric increment and relaxation time with the concentration C_p in the dilute solution and semidilute solution, we thought that the scaling behaviors are numerically more close to the Zimm dynamics model. Consequently, it can be concluded that the high-frequency relaxation was due to free counterions which fluctuate along the chain end-to-end distance R in dilute solution and within the correlation length ξ range in semidilute solution.

For the mid-frequency relaxation, all the scaling indexes of mid-frequency dielectric parameters (dielectric increment, relaxation time) with the PAA-*g*-PEO-7% solution concentration C_p were also obtained. Using different counterions species, it was proved that the mid-frequency relaxation was not due to the free counterions. Considering the scaling of both the dielectric increment and the relaxation time with the C_p in the dilute solution and semidilute solution, we thought that the mid-frequency relaxation originated from the fluctuation of condensed counterions.

The low-frequency relaxation can be attributed to interface polarization of the complex, which was formed by side-chain PEO and main-chain PAA through hydrogen bonding. By modeling the complex as a microsphere, the volume fraction ϕ of the complex was obtained by the Hanai equation.

In summary, the dynamics information on the counterion movement and the microstructure of PAA-*g*-PEO were obtained by analyzing the dielectric spectra.

By using the Eyring equation, the thermodynamic parameters, enthalpy change ΔH and entropy change ΔS, of low, mid, and high frequency were calculated from the relaxation time obtained from the temperature-dependent dielectric spectra of PAA-*g*-PEO-7% solutions. In addition, these parameters were discussed from the microscopic thermodynamical view. It was concluded that the ΔH and ΔS of low, mid, and high frequency were associated with the conformational transition of PAA-*g*-PEO-7% with the T or C_p. The dielectric studies on the temperature dependence of polyelectrolyte solution behaviors can provide an effective method to probe the microscopic thermodynamical information.

AUTHOR INFORMATION

Corresponding Author

*Tel: +861058808283. E-mail: zhaoks@bnu.edu.cn.

ACKNOWLEDGMENT

The authors thank Dr. Jinkun Hao of the Institute of Chemistry, Chinese Academy of Sciences, for providing the sample. Financial support of this work by the National Natural Science Foundation of China (No. 21173023, 20976015) is gratefully acknowledged.

REFERENCES

(1) Koper, G. J. M.; Borkovec, M. *Polymer* **2010**, *51*, 5649–5662.
(2) Schwarz, G.; Bodenthin, Y.; Geue, T.; Koetz, G.; Kurth, D. G. *Macromolecules* **2010**, *43*, 494–500.
(3) Karayianni, M.; Mountrichas, G.; Pispas, S. *J. Phys. Chem. B* **2010**, *114*, 10748–10755.
(4) Bordi, F.; Cametti, C.; Paradossi, G. *J. Phys. Chem.* **1991**, *95*, 4883–4889.
(5) Miura, N.; Shinyashiki, N.; Mashimo, S. *J. Chem. Phys.* **1992**, *97*, 8722–8726.
(6) Shinyashiki, N.; Matsumura, Y.; Mashimo, S.; Yagihara, S. *J. Chem. Phys.* **1996**, *104*, 6877–6880.
(7) Liu, C. Y.; Zhao, K. S. *Soft Matter* **2010**, *6*, 2742–2750.
(8) Lian, Y. W.; Zhao, K. S.; Yang, L. *Phys. Chem. Chem. Phys.* **2010**, *12*, 6732–6741.
(9) Barba, A. A.; et al. *J. Appl. Polym. Sci.* **2009**, *114* (2), 688–695.
(10) Yagihara, S.; Nodi, R.; Mashimo, S.; Hikichi, K. *Macromolecules* **1984**, *17*, 2700–2702.
(11) Bordi, F.; Cametti, C.; Paradossi, G. *Macromolecules* **1992**, *25*, 4206–4209.
(12) Bordi, F.; Cametti, C.; Paradossi, G. *Biopolymers* **2000**, *53*, 129–134.
(13) Bordi, F.; Cametti, C.; Paradossi, G. *Phys. Chem. Chem. Phys.* **1999**, *1*, 1555–1561.
(14) Rabiee, A. *J. Vinyl Additive Technol.* **2010**, *16*, 111–119.
(15) Bordi, F.; Cametti, C.; Gili, T.; Colby, R. H. *Langmuir* **2002**, *18*, 6404–6409.
(16) Natali, S.; Mijovic, J. *Macromolecules* **2010**, *43*, 3011–3017.
(17) Kojima, C.; Kono, K.; Maruyama, K.; Takagishi, T. *Bioconjugate Chem* **2000**, *11*, 910–917.
(18) Pan, G.; Lemmouchi, Y.; Akala, E. O.; Bakare, O. *J. Bioact. Compat. Polym.* **2005**, *20*, 113–128.
(19) Ian, G. N.; Frederick, C. S. *Biomaterials* **1995**, *16*, 617–624.
(20) Choi, H. K.; Kim, O. J.; Chung, C. K.; Cho, C. S. *J. Appl. Polym. Sci.* **1999**, *73*, 2749–2754.
(21) Chun, M. K.; Choi, H. K.; Kang, D. W.; Kim, O. J.; Cho, C. S. *J. Appl. Polym. Sci.* **2002**, *83*, 1904–1910.
(22) Serra, L.; Domenech, J.; Peppas, N. A. *Eur. J. Pharm. Biopharm.* **2006**, *63*, 11–18.
(23) Barba, A. A.; et al. *Polym. Bull.* **2009**, *62* (5), 679–688.
(24) Hao, J. K.; Yuan, G. C.; He, W. D.; Cheng, H.; Han, C. C.; Chi, Wu. *Macromolecules* **2010**, *43*, 2002–2008.
(25) Colby, R. H. *Rheol. Acta* **2010**, *49*, 425–442.

(26) Ito, K.; Hayakawa, R. *Macromolecules* **1990**, *23*, 857–862.
(27) Dobrynin, A. V.; Colby, R. H.; Rubinstein, M. *Macromolecules* **1995**, *28*, 1859–1871.
(28) Bordi, F.; Cametti, C.; Sennato, S.; Colby, R. H. *Phys. Chem. Chem. Phys.* **2006**, *8*, 3653–3658.
(29) Truzzolillo, D.; Cametti, C.; Sennato, S. *Phys. Chem. Chem. Phys.* **2009**, *11*, 1780–1786.
(30) Nagamine, Y.; Ito, K.; Hayakawa, R. *Langmuir* **1999**, *15*, 4135–4138.
(31) Nagamine, Y.; Ito, K.; Hayakawa, R. *Colloids Surf., A* **1999**, *148*, 149–153.
(32) Mafé, S.; et al. *Bioelectrochem. Bioenerg.* **1995**, *38*, 367–375.
(33) Braun, O.; Boué, F.; Candau, F. *Eur. Phys. J. E* **2002**, *7*, 141–151.
(34) Chahine, J.; Cavichiolli, F. R. *J. Phys. Chem.* **1994**, *98*, 9845–9849.
(35) Benegas, J. C.; Cesàro, A.; Rizzo, R.; Paoletti, S. *Biopolymers* **1998**, *45*, 203–216.
(36) Hanai, T.; Zhang, H. Z.; Asaka, K.; et al. *Ferroelectrics* **1988**, *86*, 191–204.
(37) Asami, K.; Irimajiri, A.; Hanai, T.; Koizumi, N. *Bull. Inst. Chem. Res.* **1973**, *51*, 231.
(38) Schwan H P. In *Physical Techniques in Biological Research*; Nastuk, W. L., Ed.; Academic Press: New York, 1963; Vol. 6, p 373.
(39) Bordi, F.; Cametti, C.; Colby, R. H. *J. Phys.: Condens. Matter* **2004**, *16*, 1423–1463.
(40) Zimm, B H. *J. Chem. Phys.* **1956**, *24*, 269–78.
(41) Manning, G. S. *J. Chem. Phys.* **1969**, *51*, 924–934.
(42) Manning, G. S. *J. Chem. Phys.* **1969**, *51*, 934–938.
(43) Doi, M.; Edwards, S. F. *Theory of Polymer Dynamics*; Clarendon Press: Oxford, UK, 1986.
(44) de Gennes, P. G. *Scaling Concepts in Polymer Physics*; Cornell University Press: Ithaca, NY, 1979.
(45) Shaw, M. T. *J. Chem. Phys.* **1942**, *10*, 609–617.
(46) Mitsumata, T.; Gong, J. P.; Ikeda, K.; Osada, Y. *J. Phys. Chem. B* **1998**, *102*, 5246–5251.
(47) Lide, D. R. *Handbook of Chemistry and Physics*, 84th ed.; CRC Press: Boca Raton, FL, 2004.
(48) Bordi, F.; Cametti, C.; Paradossi, G. *Macromolecules* **1993**, *26*, 3363–3368.
(49) Mandel, M. *Biophys. Chem.* **2000**, *85*, 125–139.
(50) Hourdet, D.; L'alloret, F.; Durand, A.; Audebert, R. *Macromolecules* **1998**, *31*, 5323–5335.
(51) Hanai, T.; Imakita, N.; Koizumi, N. *Colloid Polym. Sci.* **1982**, *260*, 1029.
(52) Hanai, T. *Kolloid Z.* **1960**, *171*, 23.
(53) Cho, J. Y.; Heuzey, M. C.; Begin, A.; Carreau, P. J. *Carbohydr. Polym.* **2006**, *63*, 507–518.
(54) De, R.; Das, B. *Eur. Polym. J.* **2007**, *43*, 3400–3407.
(55) Smith, G.; Shekunov, B. Y.; Shen, J.; Duffy, A. P.; Anwar, J.; Wakerly, M. G.; Chakrabarti, R. *Pharm. Res.* **1996**, *13*, 1181–1185.
(56) Cottet, H.; Gareil, P. *Electrophoresis* **2001**, *22*, 684–691.